Journal of Infrastructure, Policy and Development 2024, 8(13), 7836.
https://doi.org/10.24294/jipd7836

Article

Renewable energy integration impact on power quality of supply of transmission system

Oluwakemi Kehinde Akintayo*, Omowunmi Mary Longe, Oluwafemi Emmanuel Oni

Electrical and Electronic Engineering Science, University of Johannesburg, Johannesburg 2006, South Africa
*** Corresponding author:** Oluwakemi Kehinde Akintayo, kemileadcity1@gmail.com

CITATION

Akintayo OK, Longe OM, Oni OE. (2024). Renewable energy integration impact on power quality of supply of transmission system. Journal of Infrastructure, Policy and Development. 8(13): 7836. https://doi.org/10.24294/jipd7836

ARTICLE INFO

Received: 6 July 2024
Accepted: 14 September 2024
Available online: 8 November 2024

Abstract: Electrical energy is known as an essential part of our day-to-day lives. Renewable energy resources can be regenerated through the natural method within a reasonably short time and can be used to bridge the gap in extended power outages. Achieving more renewable energy (RE) than the low levels typically found in today's energy supply network will entail continuous additional integration efforts into the future. This study examined the impacts of integrating renewable energy on the power quality of transmission networks. This work considered majorly two prominent renewable technologies (solar photovoltaic and wind energy). To examine the effects, IEEE 9-bus (a transmission network) was used. The transmission network and renewable sources (solar photovoltaic and wind energy technologies) were modelled with MATLAB/SIMULINK®. The Newton-Raphson iteration method of solution was employed for the solution of the load flow owing to its fast convergence and simplicity. The effects of its integration on the quality of the power supply, especially the voltage profile and harmonic content, were determined. It was discovered that the optimal location, where the voltage profile is improved and harmonic distortion is minimal, was at Bus 8 for the wind energy and then Bus 5 for the solar photovoltaic source.

Keywords: harmonic content; harmonic distortion; load flow; Newton–Raphson; renewable energy; voltage profile

1. Introduction

Energy has a significant influence on all facets of our socio-economic life (Attabo et al., 2023). It is an indispensable component for the advancement of technology in any nation (Odesola and Ale, 2019). Renewable sources of energy have significant potential as they would close the major energy deficits if properly harnessed (Ben et al., 2021). Viable renewable sources of energy all over the world consist of solar (sun energy) photovoltaic and wind energy technologies for electric power generation (Ozioko et al., 2022).

Today, renewable energy has become a significant provider of electric power to our society; meanwhile, its integration into the power grid poses substantial practical problems to the grid especially as it relates to the voltage profile and harmonic distortion. However, solar photovoltaic and wind as a source of generating electricity provide a clean, eco-friendly, non-toxic and always obtainable source of renewable energy (Adedipe et al., 2018). While solar photovoltaic and wind energy technologies remain the most developed and economical renewable energy technologies (Ohunakin et al., 2023), the significant challenge facing their implementation, is the intermittency nature of their supply (Hanfi et al., 2020). The whole essence of linking renewable energy sources (as in this case, Solar photovoltaic and Wind) to an electric grid is to enhance the overall grid performance as it relates to power loss reduction,

improvement of voltage magnitude (profile) and ensuring that the entire grid network is stable. But at high penetration of these sources, the grid experiences power and voltage instability problems, overloading of distribution feeders, diminishing of the protective devices' ability and excessive harmonic distortion system (Anang et al., 2021).

Therefore, it becomes pertinent for electric utilities and researchers alike to examine the potential impacts of integrating renewable energy into transmission networks. This study will therefore analyze the impact of renewable energy sources integration on power quality (especially voltage profile and harmonic distortion) of transmission systems.

2. Literature review

Several research works about different integration of renewable energy sources and power quality challenges with their solutions have been reported in a great deal of scholarly literature. Thus, this section summarizes some of the works to guide upcoming investigation and engineering efforts in this critical aspect of integration. This study offers a review of power quality issues encountered due to renewable energy integration in the supply grid.

Syed et al. (2024) considered the impact of renewable sources on the electric power system. Kumar et al. (2016) reviewed the challenges connected to Renewable energy (RE) based distributed generation and solving through various custom power devices (CPD) become a very essential tool in the enhancement of power quality of supply. The challenges faced as a result of renewable energy integration were reviewed by Spoorti et al. (2018), Hossain et al. (2018), Impran et al. (2020). Tavakoli et al. (2019) carried out a detailed study of the effects of integrating both electric vehicles and solar photovoltaic into transmission networks. It was observed that separately integrating them negatively affects the stability of the power utility grid. The effects of PV (solar) integration into a distribution network were examined in Pawar and History (2019), Sharew et al. (2021), Alkawak and Ramil (2021). Sule (2022) carried out a review examining the problems associated with Renewable energy source (RES) integration as regards location, fault protection and power system stability.

Choudhury and Sahoo (2024) carried out a critical analysis of different power quality (PQ) improvement techniques in microgrids and suggested ways of mitigating PQ issues. The challenges connected with renewable energy integration and solutions to mitigate such challenges and their significant roles in the enhancement of power quality of supply were reviewed in Nirosha and Patra (2020).

From the literature, it has been established that renewable energy integration into the power grid comes with operational and technical challenges on power utility systems, as a result of the variability nature of the sources and their geographical spread (Shafie et al., 2023). There is a need for experimental studies on the effect of integrating renewable sources on power quality, especially harmonics, to suggest possible ways of mitigating the effects. This study therefore examines the integration of renewable energy sources and their effects on the power quality (harmonic distortion and voltage profile) of interconnected systems.

3. Methodology

3.1. Newton-Raphson iteration method for load–flow analysis

This numerical method makes use of the idea of successive approximation based on formerly known or presumed value and it is also based on Taylor's series expansion (Abdulkareem et al., 2021). The Newton–Raphson numerical method was adopted for this numerical analysis due to its fast rate of convergence especially for large power systems (Inyang et al., 2024), simplicity and sparsity compared to other numerical methods. In all cases, power flow computation checks bus voltage and power injected from one bus to another.

For a typical power system bus, according to Wang et al. (2010), the polar form of the nodal power equations is expressed in Equations (1) and (2).

The power equations of the bus are as given in Equation (1).

$$P_i + jQ_i = \dot{V}_i \sum_{j\in i} \hat{Y}_{ij}\hat{V}_j \; \forall j \in i (\text{where } i = 1, 2, \dots., n) \tag{1}$$

The voltage vector is given as in Equation (2).

$$\dot{V}_i = V_i e^{j\theta_i} \tag{2}$$

where V_i, θ_i represents voltage profile (magnitude) as well as the voltage phase angle respectively.

Admittance matrix elements is expressed as in Equation (3).

$$Y_{ij} = \mathrm{G}_{ij} + jB_{ij} \tag{3}$$

where G_{ij} and B_{ij} are the conductance and susceptance of a line joining two transmission stations. Separating Equation (1) into real and imaginary parts, power balance equation (real and reactive) is given as in (4) and (5) respectively.

$$0 = -P_i + V_i \sum_{j\in i} V_j\left(\mathrm{G}_{ij}\cos\theta_{ij} + jB_{ij}\sin\theta_{ij}\right) (\text{where } i = 1, 2, \dots, n) \tag{4}$$

$$0 = -Q_i + V_i \sum_{j\in i} V_j\left(\mathrm{G}_{ij}\sin\theta_{ij} - jB_{ij}\cos\theta_{ij}\right) (\text{where } i = 1, 2, \dots, n) \tag{5}$$

where: $\theta_{ij} = \theta_i - \theta_j$ represents the difference in phase angle of the voltage between buses *i* and *j*. The Equations (4) and (5) is rewritten in the form as given in Equation (6):

$$\begin{bmatrix}\Delta\theta \\ \Delta|V|\end{bmatrix} = -J\begin{bmatrix}\Delta P \\ \Delta Q\end{bmatrix} \tag{6}$$

where ΔP and ΔQ represent mismatch equations whose details are as given in Equations (7) and (8).

$$\Delta P_i = -P_i + V_i \sum_{j\in i} V_j\left(\mathrm{G}_{ij}\cos\theta_{ij} + jB_{ij}\sin\theta_{ij}\right) (\text{where } i = 1, 2, \dots, n) \tag{7}$$

$$\Delta Q_i = -Q_i + V_i \sum_{j\in i} V_j\left(\mathrm{G}_{ij}\sin\theta_{ij} - jB_{ij}\cos\theta_{ij}\right) (\text{where } i = 1, 2, \dots, n) \tag{8}$$

J represents the Jacobian matrix (partial derivatives) as depicted in Equation (9):

$$\begin{bmatrix} \frac{\partial \Delta P}{\partial \theta} & \frac{\partial \Delta P}{\partial |V|} \\ \frac{\partial \Delta Q}{\partial \theta} & \frac{\partial \Delta Q}{\partial |V|} \end{bmatrix} \tag{9}$$

Therefore, the obtained system of equation is then solved in order to obtain the next guess as given in Equations (10) and (11).

$$\theta^{m+1} = \theta^{m} + \Delta\theta \tag{10}$$

$$|V|^{m+1} = |V|^{m} + \Delta|V| \tag{11}$$

The iteration continues until a common termination condition is met where mismatch equations is less than a given tolerance, ε.

i.e., $\Delta P_i^{(r)} < \varepsilon, \Delta Q_i^{(r)} < \varepsilon$

The Flow chart describing the Newton-Raphson (N-R) load flow algorithm procedure MATLAB/SIMULINK® is depicted in **Figure 1**.

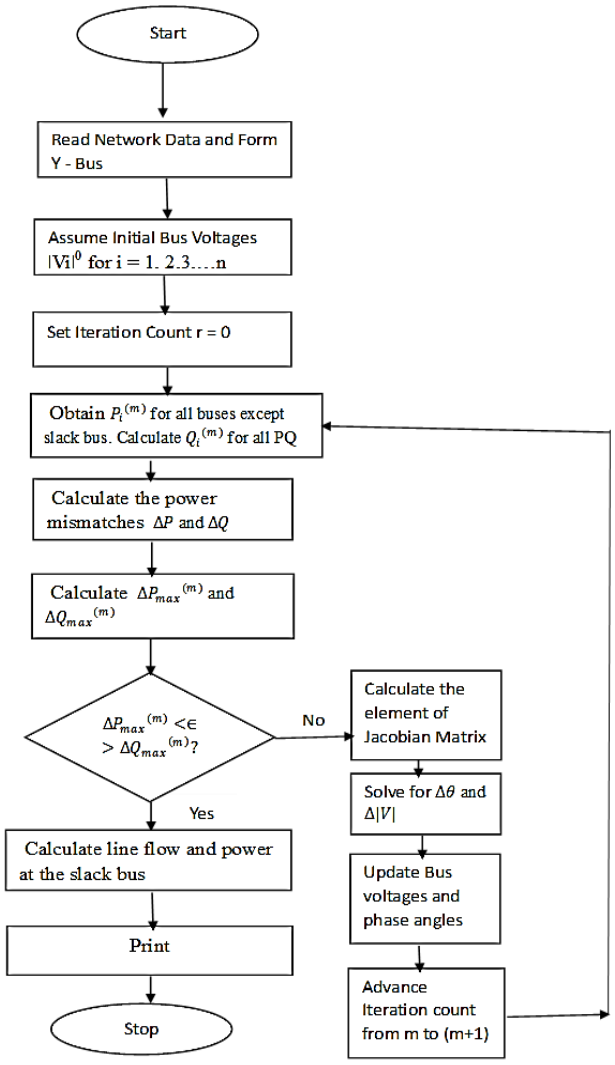

Figure 1. Flow chart describing Newton-Raphson iteration precedure.

3.2. Total harmonic distortion (THD)

As given in Equation (12), THD helps to describe the measure of harmonic distortion content existing in a signal.

$$THD = \frac{\sqrt{V_2^2 + V_3^2 + V_4^2 + \ldots V_n^2}}{V_s} \tag{12}$$

where V_s—amplitude of the source voltage, V_2—second harmonic voltage amplitude and V_n—*n*-th harmonic voltage amplitude. Note: All the voltages are Root-Mean-Square (RMS) Values.

3.3. System description and modeling of the test network (IEEE 9-bus)

This is an electric power transmission network of 230 kV capacity. It is a three-machine, nine-bus system (Jena et al., 2018). It consists of three synchronous generators (Bus 1 taken as the reference/slack/swing), nine buses, three-two winding transformers, six transmission lines and three PQ loads (Illinois, 2022). The test system was modeled using MATLAB/SIMULINK® software as shown in **Figure 2** with details in Appendix A–F.

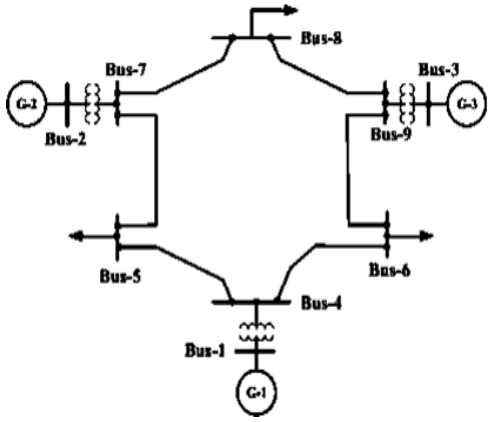

(a)

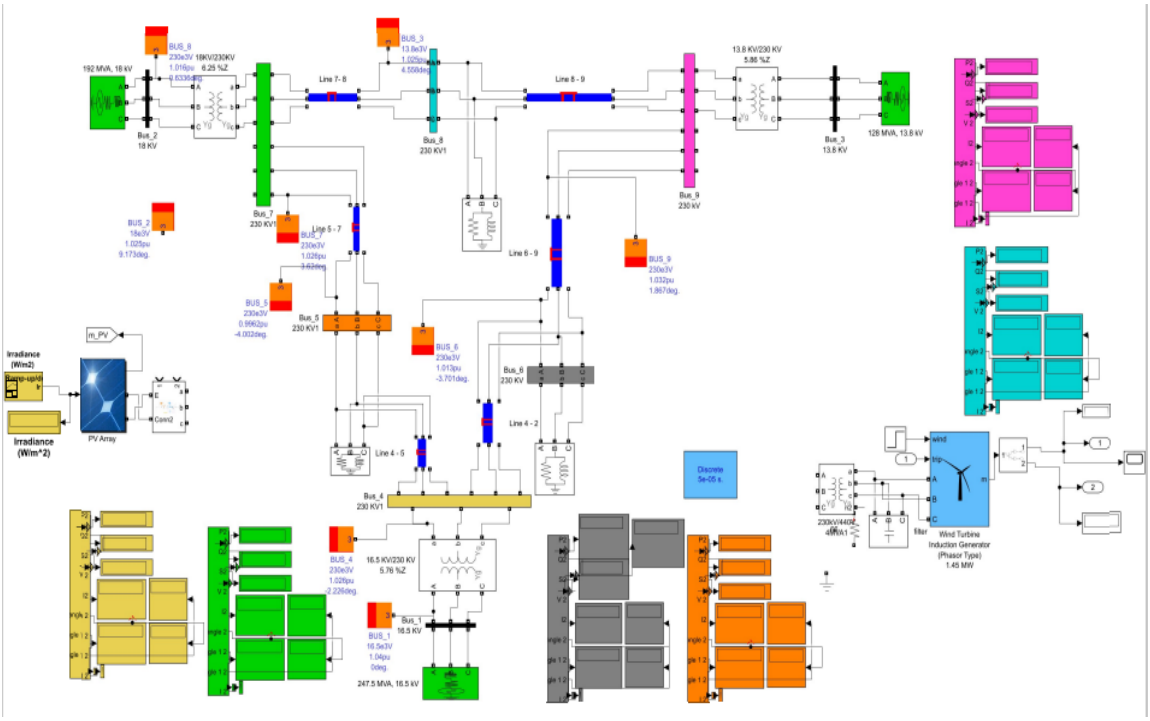

(b)

Figure 2. Modeled test system: **(a)** One line diagram of the IEEE 9-bus test system; **(b)** IEEE 9-bus model in MATLAB/SIMULINK.

3.4. Modelling of the wind and solar photovoltaic energy sources

The main formula describing the wind energy conversion process is given in Equation (13) (Wagner and Mathur, 2020).

$$P_w = \frac{1}{2} C_p(\lambda, \beta) \rho A V_w^3 \tag{13}$$

where A is the area of the blade, C_p is the wind power coefficient (this depends on Tip speed ratio λ and pitch angle β. Tip speed ratio $\lambda = {R\omega_r}/{V}$, where ω_r is the rotor speed.

$A = \pi R^2$, ρ density of the air, P_w is the output power of the wind turbine and V is the speed of the wind, R is the radius of the rotor blade.

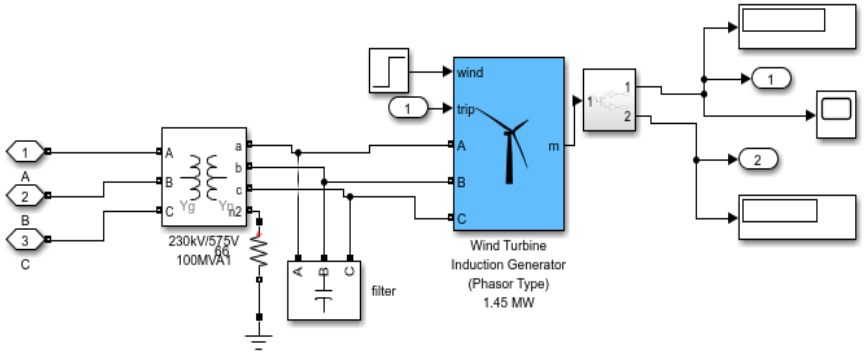

Figure 3. The wind power system in MATLAB/SIMULINK®.

Figure 3 describes the diagram, in MATLAB/SIMULINK®, of the wind power system. Similarly, **Figure 4**, describes the diagram of the solar photovoltaic system in MATLAB/SIMULINK® as well as the equivalent circuit diagram.

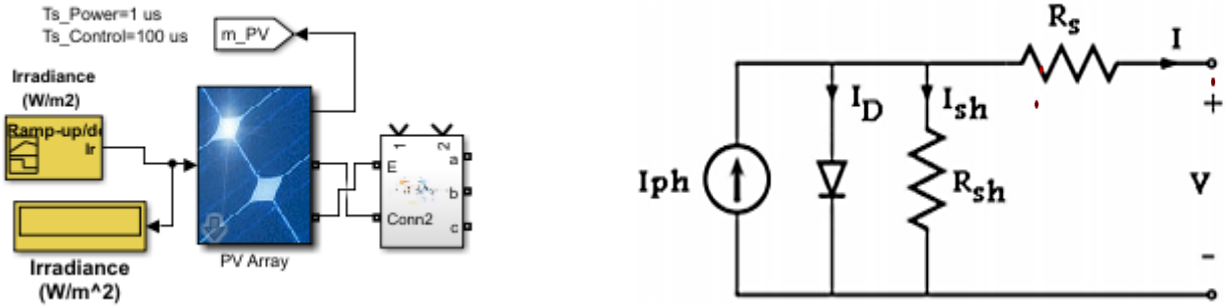

(a) **(b)**

Figure 4. Diagram of the solar photovoltaic system: **(a)** solar photovoltaic in MATLAB/SIMULINK; **(b)** equivalent circuit solar photovoltaic cell.

The characteristic equations for the modeled solar photovoltaic cell (Makanju and Oluwalana, 2020) is given in Equations (14)–(18):

$$I_{rs} = \frac{I_{sc}}{Exp^{\left(\frac{q.v_{oc}}{nN_sKT}\right)-1}} \tag{14}$$

$$I_0 = I_{rs} \cdot \left(\frac{T}{T_n}\right)^3 Exp\left[\frac{qE_{go}\left(\frac{1}{T_n}-\frac{1}{T}\right)}{n.k}\right] \tag{15}$$

$$I_{sh} = \frac{V + I.R_s}{R_{sh}} \tag{16}$$

$$I_{ph} = [I_{sc} + K_i(T - 298)]\frac{G}{1000} \tag{17}$$

$$I = I_{ph} - I_0\left[Exp^{\left(\frac{q.(V+I.R_s)}{nN_sKT}\right)-1}\right] - I_{sh} \tag{18}$$

where I is the output current, I_{ph} is the photocurrent of the PV cells, Ish is the shunt current, K is the Boltzmann's constant, I_{sc} is the short circuit current, G is the solar Irradiance, R is the shunt resistance, T is the cell temperature, I_{rs} is the reverse saturation current, I_{sh} is the current through shunt resistor, V_{oc} is the open circuit voltage, V_t is the diode thermal voltage, N is the number of PV module, n is the ideality factor, E_{go} is the energy band gap of the semiconductor, q is the charge.

The MATLAB/SIMULINK® software was employed in the modelling of the wind and solar photovoltaic energy sources. The modelled wind energy system consists of a constant (fixed) wind turbine system of 575 V and a power rating of 100 MVA. A 100 MVA, 575V/230 kV three-phase, two-winding coupling transformer was used for connecting the wind system to the test network. Similarly, the solar panel

consists of 5 series-connected modules of 66 strings each. A module consists of 96 series-connected cells each. The module has an open-circuit voltage value of 64.2 V and a short–circuit current of 5.96 A. The PV array is expected to deliver a maximum power of 100kW at 1000W/m^2 solar irradiance.

A 5 kHz DC-DC converter was employed to increase the nominal voltage of the photovoltaic from 273 Vdc to 500 Vdc. Extraction of the maximum power was made possible by employing an MPPT controller which automatically varies the duty cycle generating the maximum voltage. A 3-level, Voltage Source Converter (VSC) was employed to convert the voltage level (the 500 Vdc link) to 260 Vac at a power factor of unity. A capacitor bank (10 kVar) was used in harmonic filtering produced by VSC. A 100 kVA, 260V/230kV three-phase and two-winding transformer was employed for connecting the Photovoltaic (PV) system to the test network. The load flow of the simulation of the test network was done. The voltage profile and the harmonics contents were recorded.

4. Results and discussion

For the effective study of the effects of renewable energy integration on transmission networks, the IEEE 9-Bus, a transmission network system was used for the study. The test network was modelled with the aid of MATLAB/SIMULINK software®. Renewable energy sources were also modelled and incorporated into the network.

4.1. Scenario 1 (base case): No renewable energy source integration on the IEEE 9-bus load flow simulation

Results from the simulation of the load flow of the test system carried out (without integrating the renewable energy sources) are as shown in **Figure 5**. The magnitude of the voltage profile per unit (p.u.) values falls within the permissible limit of $1.00 \pm 5\%$ p.u. The total harmonic distortion at this base case was seen to be 0.00% as depicted in **Table 1**.

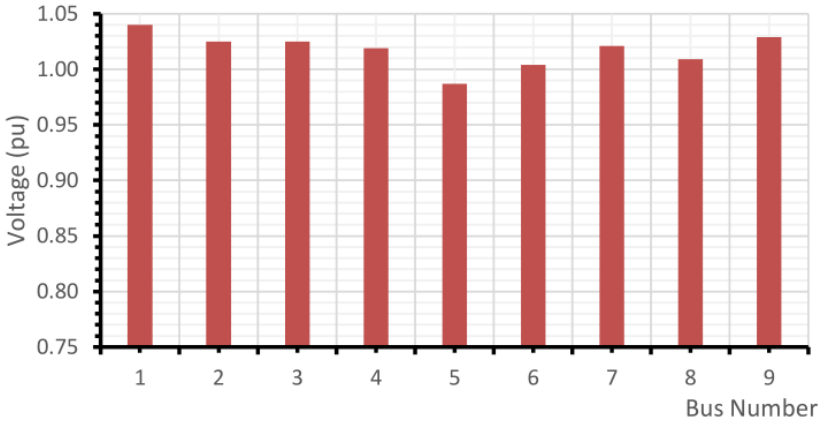

Figure 5. The magnitude of voltage (p.u.) with no RES integrated.

Table 1. Total hamonic distortion of the scenarios.

Bus number	Base case (THD before integration (%)	THD after wind integration (%)	THD after solar PV integration (%)
Bus 5	0.00	0.29	2.15
Bus 6	0.00	0.27	2.22
Bus 8	0.00	0.20	2.45

4.2. Scenario 2: Integration of wind energy source

To get the effect of wind energy integration, the modelled wind turbine was placed in all the load buses one after the other and the simulations of the load flow of the test system with wind energy source integrated were carried out in each case. **Figures 6**–**8** give the voltage profile of the network at buses 5, 6 and 8 in comparison with the base case. It was discovered that there exists a slight variation in the other buses, although none of the buses falls outside the permissible limit of $1.00 \pm 5\%$ p.u. From the simulation results, in comparison with the base case scenario (i.e., no renewable source integrated), the wind source integration at Bus 8 gave the most appropriate output in terms of having the least harmonic distortion, as shown in **Figures 9**–**11**.

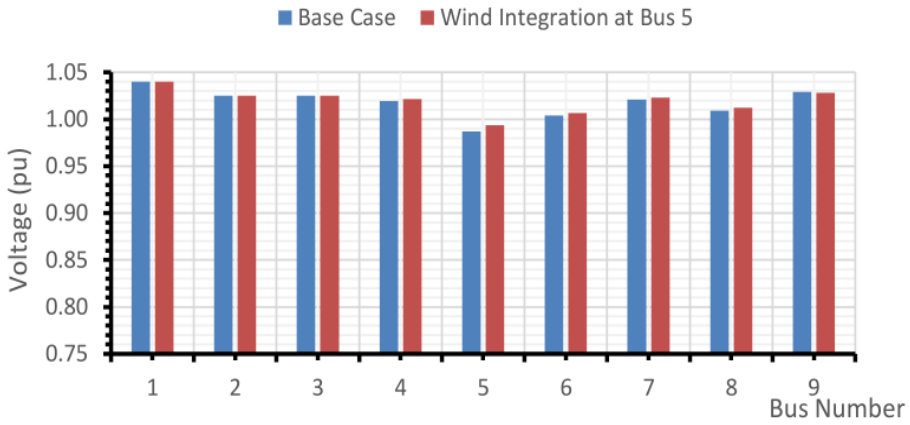

Figure 6. The magnitude of voltage (p.u.) with wind energy integration at Bus 5.

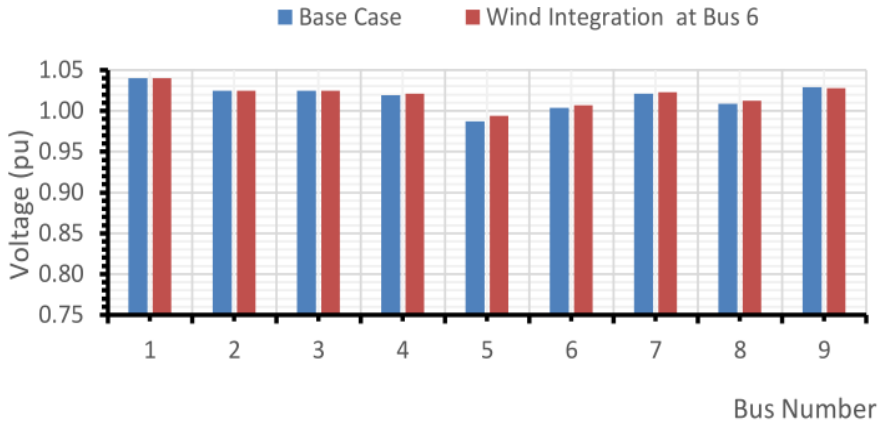

Figure 7. The magnitude of Voltage (p.u.) with wind energy integration at Bus 6.

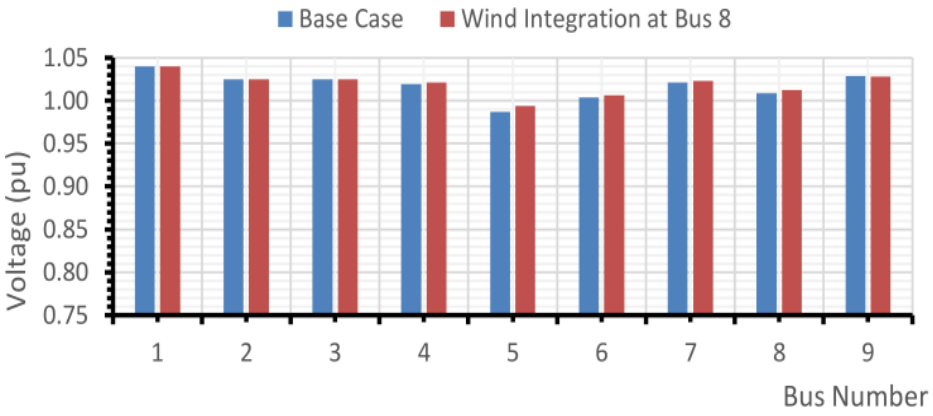

Figure 8. The magnitude of voltage (p.u.) with wind energy integration at Bus 8.

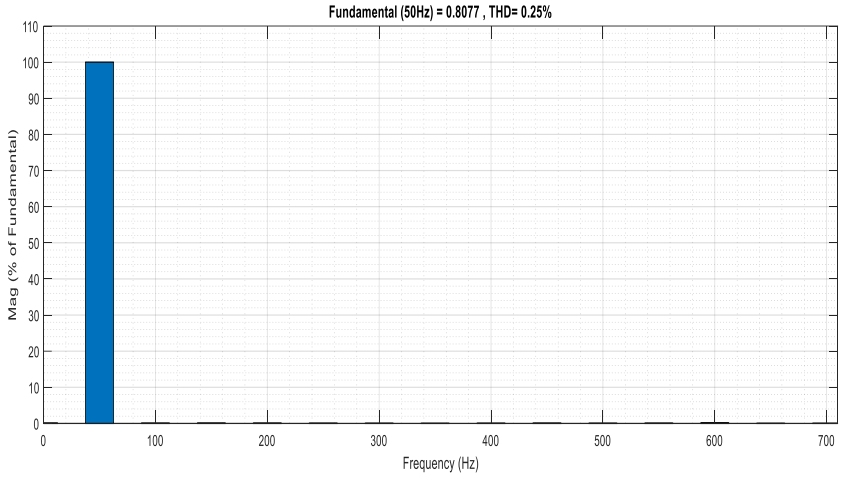

Figure 9. THD (voltage) values with wind energy integration at Bus 5.

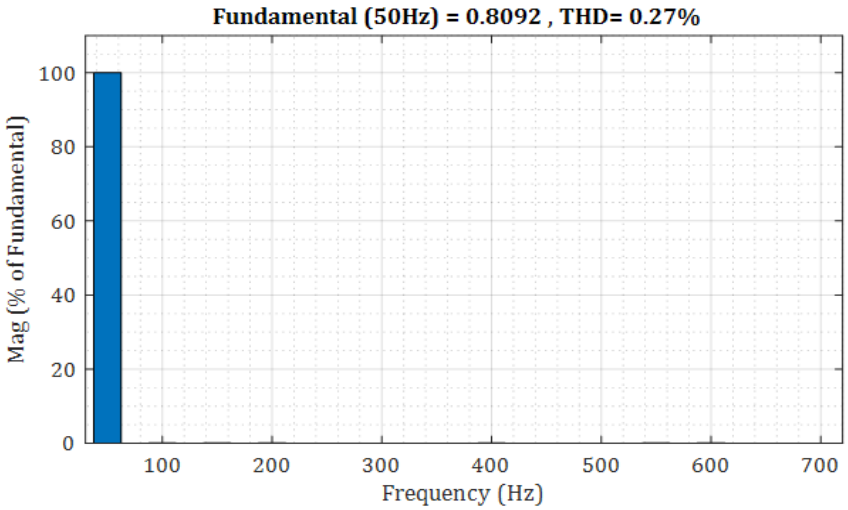

Figure 10. THD (voltage) values with wind energy integration at Bus 6.

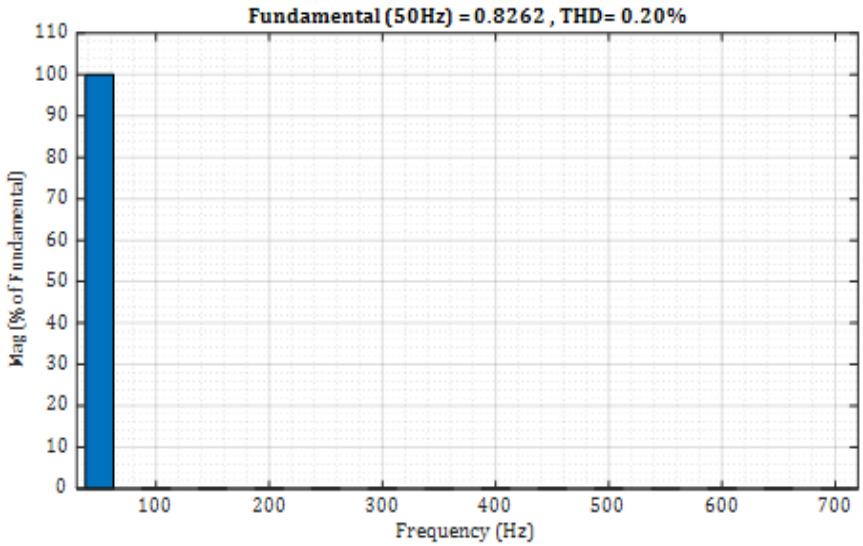

Figure 11. THD (voltage) values with wind energy integration at Bus 8.

4.3. Scenario 3: Integration of solar energy source

The modelled Solar photovoltaic module was placed in all the load buses one after the other and the simulation of the load flow of the test system with solar energy source integrated was carried out in each case. From the simulation results of the load flow and the harmonics analysis, compared with the base case scenario (i.e., no renewable integrated), the solar source integration at Bus 5 gave the most appropriate output, as shown in the voltage profile in **Figures 12**–**14**. It was discovered that there exists a slight variation in the other buses, although none of the buses falls outside the permissible limit of 1.00 ± 5% p.u. The THD graph are as depicted in **Figures 15**–**17**.

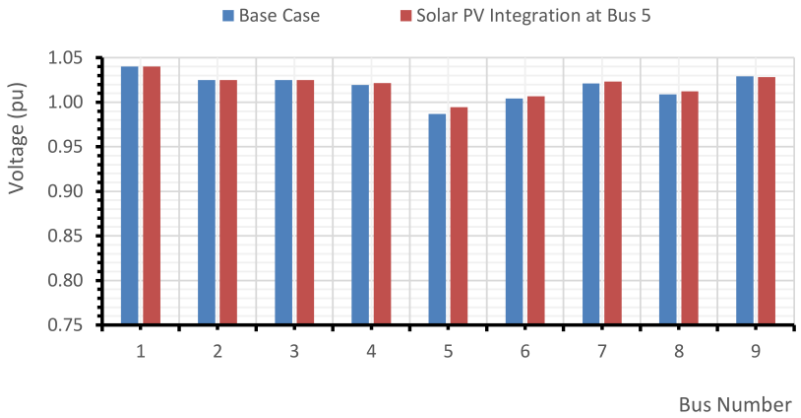

Figure 12. The magnitude of voltage (p.u.) with solar PV integration at Bus 5.

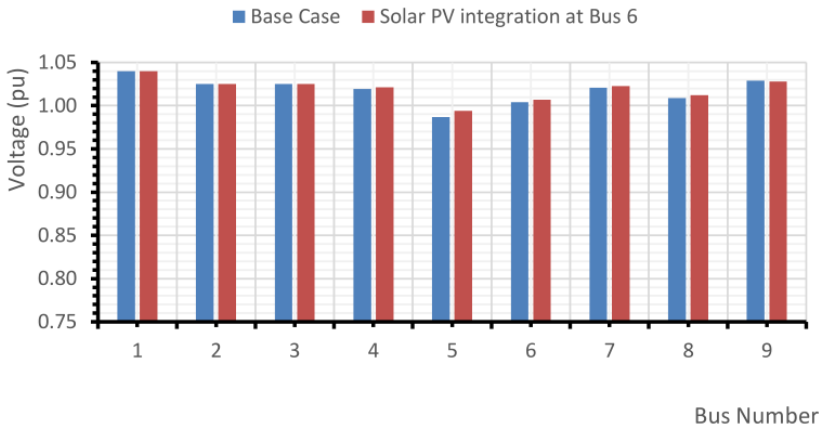

Figure 13. The magnitude of voltage (p.u.) with solar PV integration at Bus 6.

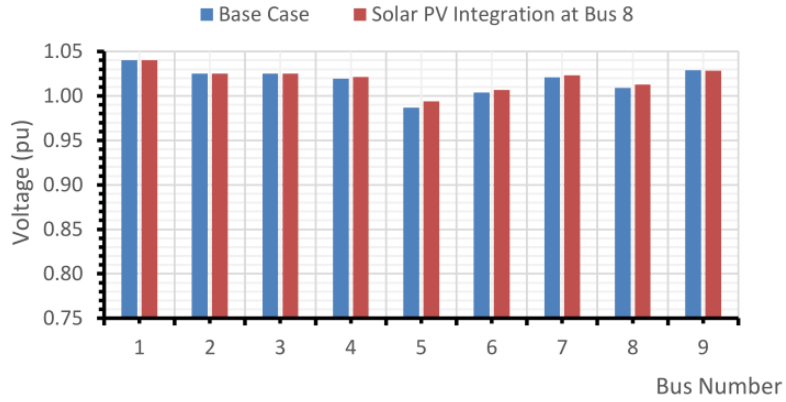

Figure 14. The magnitude of voltage (p.u.) with solar PV integration at Bus 8.

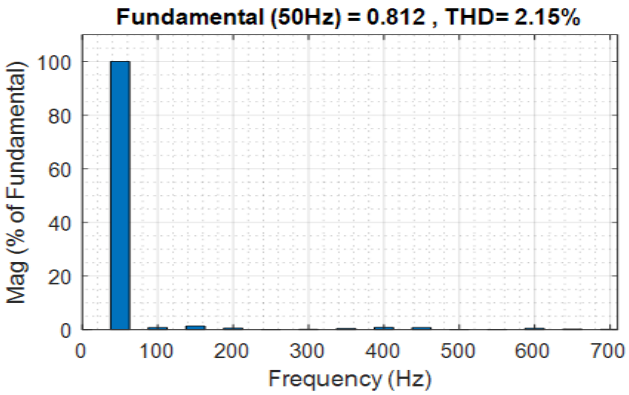

Figure 15. THD (voltage) values with solar PV integration at Bus 5.

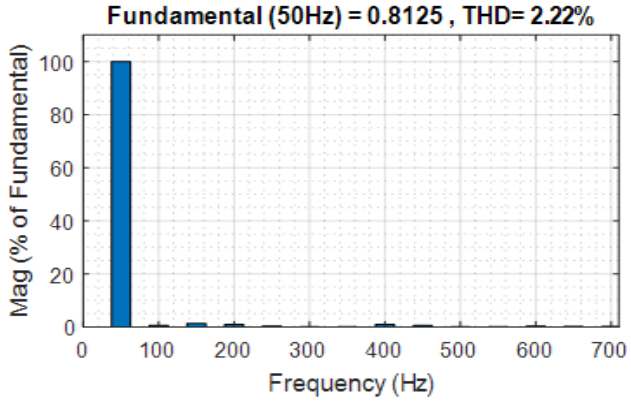

Figure 16. THD (voltage) values with Solar PV integration at Bus 6.

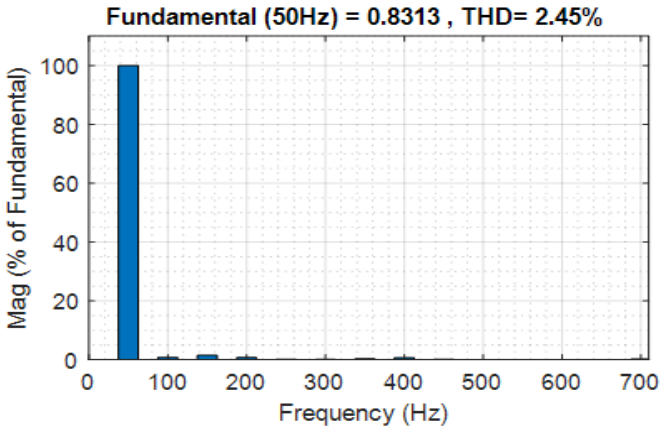

Figure 17. THD (voltage) values with solar PV integration at Bus 8.

5. Conclusion

In this work, two major renewable energy sources (wind energy source and solar photovoltaic) have been integrated into the transmission network (IEEE 9-Bus). The test system (IEEE 9-Bus) and the renewable energy sources were modelled with MATLAB/SIMULINK®. The Newton-Raphson iteration method of solution was employed for the solution of the load flow owing to its fast convergence and simplicity. The effects of its integration on the quality of the power supply, especially the voltage profile and harmonic content, were determined. It was discovered that the optimal location, where the voltage profile is improved and harmonic distortion is minimal, was at Bus 8 for the wind energy and then Bus 5 for the solar photovoltaic source. Further studies may investigate the:

- Effects of dynamic load on the performance of renewable energy.
- Level of renewable energy penetration and the corresponding effects on power quality.
- The cost-effectiveness of integrating renewable energy.
- Resilience of the grid when renewable energy and electric vehicles are integrated.
- Addition of Filter.
- Experimental validation.

Author contributions: Conceptualization, OKA, OML and OEO; methodology, OKA, OML and OEO; software, OKA, OML and OEO; validation, OKA, OML and

OEO; formal analysis, OKA, OML and OEO, data curation, OKA; writing—original draft preparation, OKA; writing—review and editing, OKA, OML and OEO; visualization, OKA, OML and OEO; supervision, OKA, OML and OEO; funding acquisition, OKA, OML and OEO. All authors have read and agreed to the published version of the manuscript.

Funding: This research is funded by the National Research Foundation, South Africa with grant reference SRUG2205025715.

Conflict of interest: The authors declare no conflict of interest.

References

Abdulkareem, A., Somefun, T. E., Awosope, C. O. A., et al. (2021). Power system analysis and integration of the proposed Nigerian 750-kV power line to the grid reliability. SN Applied Sciences, 3(12). https://doi.org/10.1007/s42452-021-04847-3

Adedipe, O., Abolarin, M. S., & Mamman, R. O. (2018). A Review of Onshore and Offshore Wind Energy Potential in Nigeria. IOP Conference Series: Materials Science and Engineering, 413, 012039. https://doi.org/10.1088/1757-899x/413/1/012039

Alkawak, O. A., & Ramil, A. R. (2021). Impact of Renewable Energy Sources Integration with Power Grid Systems Through Several Methodologies. International Journal of Nonlinear Analysis and Application, 12, 2333–2344.

Anang, N., Syd Nur Azman, S. N. A., Muda, W. M. W., et al. (2021). Performance analysis of a grid-connected rooftop solar PV system in Kuala Terengganu, Malaysia. Energy and Buildings, 248, 111182. https://doi.org/10.1016/j.enbuild.2021.111182

Attabo, A. A., Ajayi, O. O., Oyedepo, S. O., et al. (2023). Assessment of the wind energy potential and economic viability of selected sites along Nigeria's coastal and offshore locations. Frontiers in Energy Research, 11. https://doi.org/10.3389/fenrg.2023.1186095

Ben, U. C., Akpan, A. E., Mbonu, C. C., et al. (2021). Integrated technical analysis of wind speed data for wind energy potential assessment in parts of southern and central Nigeria. Cleaner Engineering and Technology, 2, 100049. https://doi.org/10.1016/j.clet.2021.100049

Choudhury, S., & Sahoo, G. K. (2024). A critical analysis of different power quality improvement techniques in microgrid. E-Prime—Advances in Electrical Engineering, Electronics and Energy, 8, 100520. https://doi.org/10.1016/j.prime.2024.100520

Hanifi, S., Liu, X., Lin, Z., et al. (2020). A Critical Review of Wind Power Forecasting Methods—Past, Present and Future. Energies, 13(15), 3764. https://doi.org/10.3390/en13153764

Hossain, E., Tur, M. R., Padmanaban, S., et al. (2018). Analysis and Mitigation of Power Quality Issues in Distributed Generation Systems Using Custom Power Devices. IEEE Access, 6, 16816–16833. https://doi.org/10.1109/access.2018.2814981

Illinois Centre for a Smarter Electric Grid. (2022). Publicly available power flow and transient stability cases. Illinois: Illinois Centre for a smarter Electric Grid.

Impram, S., Varbak-Nese, S., & Oral, B. (2020). Challenges of renewable energy penetration on power system flexibility: A survey. Energy Strategy Reviews, 31, 100539. https://doi.org/10.1016/j.esr.2020.100539

Inyang, P. J., Nkan, I., & Okpo, E. E. (2024). Voltage Stability Improvement in the Nigerian Southern 330kV Power System Network with UPFC FACTS Devices. American Journal of Engineering Research, 9(7), 27–33.

Jena, R., Chirantan, S., Swain, S. C., et al. (2018). Load flow analysis and optimal allocation of SVC in nine bus power system. 2018 Technologies for Smart-City Energy Security and Power (ICSESP). https://doi.org/10.1109/icsesp.2018.8376741

Kumar, V., Pandey, A. S., & Sinha, S. K. (2016). Grid integration and power quality issues of wind and solar energy system: A review. In: Proceedings of the 2016 International Conference on Emerging Trends in Electrical Electronics & Sustainable Energy Systems (ICETEESES). pp. 71–80.

Makanju, T. D., & Oluwalana, O. J. (2020). A Novel Methodology For Modelling PV Module Based on Monitored Data. Journal of Multidisciplinary Engineering Science Studies JMESS, 6(3), 3072–3076.

Nirosha, C., & Patra, P. S. K. (2020). Power Quality Issues of Wind and solar Energy Systems integrated into the Grid. Journal of Computational and Theoretical Nanoscience, 26(5), 514–523.

Odesola, A. O., & Ale, T. O. (2019). Overview of energy generation at Jebba Hydropower Station (2009–2016). Nigerian Journal of Technology, 38(3), 744. https://doi.org/10.4314/njt.v38i3.28

Ohunakin, O. S., Matthew, O. J., Adaramola, M. S., et al. (2023). Techno-economic assessment of offshore wind energy potential

at selected sites in the Gulf of Guinea. Energy Conversion and Management, 288, 117110. https://doi.org/10.1016/j.enconman.2023.117110

Ozioko, I. O., Ugwuanyi, N. S., Ekwue, A. O., et al. (2022). Wind energy penetration impact on active power flow in developing grids. Scientific African, 18, e01422. https://doi.org/10.1016/j.sciaf.2022.e01422

Panda, R. P., Sahoo, P. K., & Satpathy, P. K. (2015). A Novel Scheme for Placement and Sizing of SVCs to Improve Voltage Stability of Wind—Integrated Power Systems. International Journal of Renewable Energy Research, 5(2), 452–463.

Pawar, S., & History, M. (2019). Harmonic Analysis of High Penetration PV Systems on Distribution Network. International Journal of Applied Engineering Research, 6(6), 401–408.

Shafiee, M., Sajadinia, M., Zamani, A. A., et al. (2024). Enhancing the transient stability of interconnected power systems by designing an adaptive fuzzy-based fractional order PID controller. Energy Reports, 11, 394–411. https://doi.org/10.1016/j.egyr.2023.11.058

Sharew, E. A., Kefale, H. A., & Werkie, Y. G. (2021). Power Quality and Performance Analysis of Grid-Connected Solar PV System Based on Recent Grid Integration Requirements. International Journal of Photoenergy, 2021, 1–14. https://doi.org/10.1155/2021/4281768

Spoorti, S. N., Gowda, T. R., & Sridhar, N. H. (2018). Emerging Power Quality Challenges due to Integration of Solar and Wind Energy Sources. International Journal of Scientific Development and Research, 3(5), 277–282.

Sule, A. H. (2022). Impact of Integration of Renewable Energy Sources on Power System Stability, Fault Protection and Location: A Review. Direct Research Journal of Engineering and Information Technology, 9(4), 87–100.

Syed, M. S., Suresh, C. V., & Sivanagaraju, S. (2024). Impact of Renewable Sources on Electrical Power System. Journal of Operation and Automation in Power Engineering, 261–268.

Tavakoli, A., Sah, S., Arif, M. T., et al. (2019). Impacts of Grid Integration of Solar PV and Electric Vehicle on Grid Stability Power Quality and Energy Economics: A Review. IET Energy Systems Integration, 1–18.

Wagner, H. J. & Mathur, J. (2020). Introduction to Wind Energy Systems: Basics, Technology and Operation. Berlin: Springer - Verlag.

Wang, X., Yonghua, S., & Malcom, I. (2010). Modern Power Systems Analysis. New York: Springer.

Appendix A: Data used for IEEE 9-bus model

Table A1. Slack generator data.

Bus	Power rating (MVA)	Voltage rating (kV)	Voltage (p.u.)	Phase angle (°)	Active power (MW)	Reactive power (MVar)
1	247.5	16.50	1.040	0.00		

Table A2. PV generator data.

Bus	Power rating (MVA)	Voltage rating (kV)	Voltage (p.u.)	Phase angle (°)	Active power (MW)	Reactive power (MVar)
2	192.0	18.00	1.025	0.00	163	0
3	128	13.80	1.025	0.00	85	0

Table A3. Load bus data.

Bus	Power rating (MVA)	Voltage rating (kV)	Voltage (p.u.)	Phase angle (°)	Active power (MW)	Reactive power (MVar)
5	100	230	1.00	0.00	125	50
6	100	230	1.00	0.00	90	30
8	100	230	1.00	0.00	100	35

Table A4. Other bus data.

Bus	Power rating (MVA)	Voltage rating (kV)	Voltage (p.u.)	Phase angle (°)	Active power (MW)	Reactive power (MVar)
4	100	230	1.00	0.00		
7	100	230	1.00	0.00		
9	100	230	1.00	0.00		

Table A5. Transformer data.

From bus	To bus	Power rating (MVA)	Voltage rating (kV)	Frequency (Hz)	Voltage ratio	R (p.u.)	X (p.u.)
1	4	100	230	50	14	0.0	0.0576
2	7	100	230	50	13	0.0	0.0625
3	9	100	230	50	13	0.0	0.0586

Table A6. Line data.

From bus	To bus	R (p.u.)	X (p.u.)
4	5	0.0529	0.001192
4	6	0.08993	0.001290
5	7	0.16928	0.002259
6	9	0.20631	0.002380
7	8	0.044965	0.001010
8	9	0.062951	0.001414

Appendix B

Table B1. List of abbreviations.

FFT	Fast fourier transform
HEV	Hybrid electric vehicle
ICEV	Internal combustion engine vehicle
IEEE	Institution of electrical and electronics engineering
PHEV	Plug—in hybrid electric vehicle
PQ	Power quality
PQD	Power quality disturbance
PV	Photovoltaic
RE	Renewable energy
RES	Renewable energy sources
THD	Total harmonic distortion
VSC	Voltage source converter
WF	Wind farm
WSCC	Western system coordinating council

Appendix C

Table C1. Table of works comparison.

No	Author(S) and year	Works	Gap
1	Syed et al. (2024)	Considered the impact of renewable sources on the electric power system.	Impact of renewable sources was considered
3	Spoorti et al. (2023)	The challenges faced as a result of renewable energy integration were reviewed.	Only review was carried out
4	Tavakoli et al. (2020)	Effects of integrating both electric vehicles and solar photovoltaic into transmission networks.	Solar PV and EV integration was carried out.
5	Sule (2022)	A review examining the problems associated with Renewable energy source (RES) integration as regards location, fault protection and power system stability.	Only a review carried out
6	Choudhury and Sahoo (2024)	A critical analysis of different power quality (PQ) improvement techniques in microgrids and suggested ways of mitigating PQ issues.	PQ improvement techniques carried out
7	Nirosha and Patra (2020)	The challenges connected with renewable energy integration and solutions to mitigate such challenges and their significant roles in the enhancement of power quality of supply were reviewed.	A review carried out

Appendix D: DC-DC conversion formula

The output voltage of buck DC/DC converters is expressed as $V_{out} = V_{in} \times \left(T_{on}/\left(T_{on} + T_{off}\right)\right)$, where $\left(T_{on}/\left(T_{on} + T_{off}\right)\right)$ is the duty ratio, V_{out} is the output voltage, V_{in} is the input voltage.

Appendix E

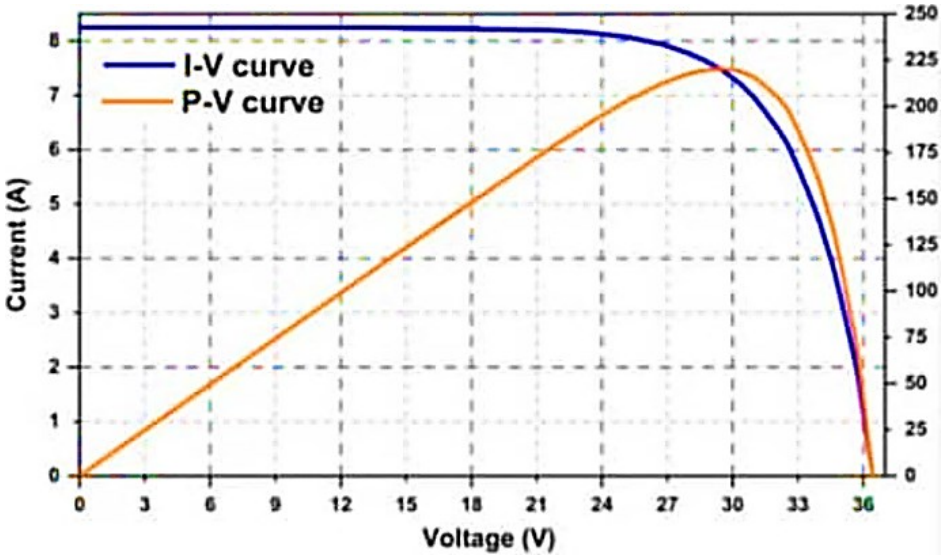

Figure E1. I-V and P-V characteristics of a PV module at STC.